*Eur J Med Chem* (1996) 31, 23–35




# Synthesis, structural characterization and cytotoxic effect of 6-amino-6-deoxy-L-ascorbic acid derivatives

M Kralj[1], B Kojić-Prodić[1]*, Z Banić[2], M Grdiša[1], V Vela[2], B Šušković[2], K Pavelić[1]

[1]*Rudjer Bošković Institute, Bijenička cesta 54, POB 1016, HR-10001 Zagreb;*
[2]*Pliva - Research Institute, Prilaz baruna Filipovića 25, HR-10000 Zagreb, Croatia*

(Received 30 June 1995; accepted 12 September 1995)

**Summary** — The synthesis, extended molecular modelling and cytotoxic effects of 6-amino-6-deoxy-L-ascorbic acid derivatives are described. For structure–function considerations, comparative conformational analysis was performed and X-ray structure analysis, molecular mechanics and molecular dynamics simulations were used in the search for the bioactive conformation(s). The cytotoxic effect of *N,N*-dimethyl-6-amino-6-deoxy-L-ascorbic acid on human tumour cell lines (Hep2, MiaPaCa2, HeLa) and on diploid human fibroblast (WI 38) was examined. The dimethylamino derivative of ascorbic acid expressed a stronger cytotoxic effect than ascorbic acid itself. This effect was cell-specific and dose dependent. The treatment of the cells with *N,N*-dimethyl-6-amino-6-deoxy-L-ascorbic acid probably resulted in apoptosis, evidenced by characteristic morphological changes and ladder DNA fragmentation. Apoptosis was not mediated by c-Myc or p53 proteins.

**ascorbic acid derivative / synthesis / X-ray structure analysis / molecular modelling / cytotoxic effect**

## Introduction

Ascorbic acid **1** (chart 1) plays a role in many biochemical processes and it is essential for normal functioning of a living organism. It is generally non-toxic, but in high concentrations it has a cytotoxic effect on some cells *in vitro* and *in vivo* [1–3]. Therefore, it can be used as a model to study antitumour activities. It is expected that introduction of some specific substituents into the ascorbic acid molecule would enhance its cytotoxic (antitumour) activity, while the human body could still tolerate such a modified molecule. In some recent investigations of the biological activity of ascorbic acid and its derivatives, it has been found that the replacement of a hydroxy group at the C6 atom by bromine leads to enhanced antitumour activity against mouse melanoma cells *in vitro* and *in vivo* [4]. This observation has led to the synthesis of new amino ascorbic acid derivatives and screening for their cytotoxic (antitumour) activity. On the route to produce more active analogues by chemical modifications of the parent compound (scheme 1), a search for bioactive conformation(s) is an essential step. The conformational analysis of a side chain, in neutral molecules and zwitterions, is focused on finding bioconformer(s) of 6-amino-6-deoxy-L-ascorbic acid **2** and *N,N*-dimethyl-6-amino-6-deoxy-L-ascorbic acid **3**. In this study we report the synthesis of *N,N*-dimethyl-6-amino-6-deoxy-L-ascorbic acid **3** and *N*-methyl-6-amino-6-deoxy-L-ascorbic acid **4** and the possible mechanism of the cytotoxic effect on several human tumour cell lines.

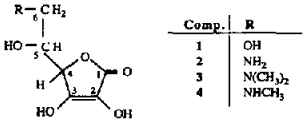


| Comp. | R |
|---|---|
| 1 | OH |
| 2 | $NH_2$ |
| 3 | $N(CH_3)_2$ |
| 4 | $NHCH_3$ |

**Chart 1.** Chemical structure of the compounds studied.

*Correspondence and reprints

## Results

### *Synthesis*

The formulae of the compounds discussed are presented in chart 1 and synthetic routes in scheme 1.

The reaction of primary amine with formaldehyde under a reductive conditions is frequently used as a method for the preparation of dimethylamine [5–14].

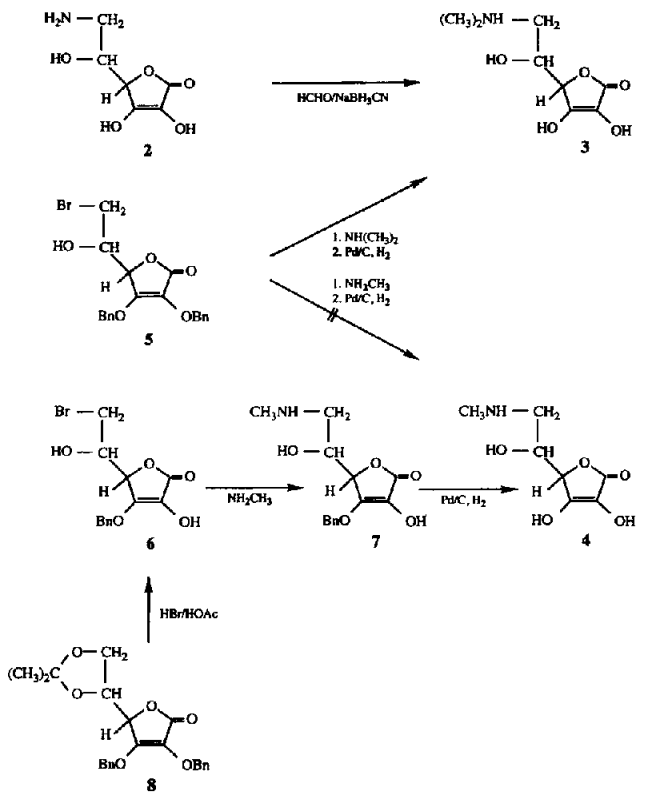

**Scheme 1.** Synthetic routes.

*N,N*-Dimethyl-6-amino-6-deoxy-L-ascorbic acid **3** was obtained by condensation of **2** with formaldehyde in an aqueous acid medium with sodium cyanoborohydride as a reductive agent. Both reagents were used in a stoichiometric excess over the amount of **2**. The molecule was structurally characterized by the X-ray diffraction method. In the crystalline state, the molecule appears as a zwitterion formed by dissociation of the proton at the $O^3$ position.

*N*-Monomethylation of primary amines is often encountered in organic synthesis. Although a great number of methods have been described, none is without limitations [15–18]. The mechanism of reductive methylation of the primary amine in an aqueous acidic medium has been proposed and experimentally supported [9]. In the first stage it implies the formation of monomethylamine. By increasing the ratio of amine to reducing agent, some of the reactions have been controlled successfully. In our case, *N*-methyl-6-amino-6-deoxy-L-ascorbic acid **4** was formed together with *N,N*-dimethyl-6-amino-6-deoxy-L-ascorbic acid **3** when a double stoichiometric quantity of **2** and formaldehyde to sodium cyanoborohydride was used. By chromatographic purification on a silica-gel column a small amount of **4** was obtained. Thus, a reaction with better yield of **4** was developed.

Alkylation of dimethylamine or methylamine with 6-bromo-6-deoxy-L-ascorbic acid appeared to be a possible method for the preparation of **3** and **4**, respectively. The hydroxy groups of enediol lactone in positions C2 and C3 are very reactive in alkaline medium and they should be protected prior to the reaction. As the most suitable substance 6-bromo-6-deoxy-$O^2$,$O^3$-dibenzyl-L-ascorbic acid **5** was used [19] to obtain **3** and **4**; alkylation of dimethylamine followed by *in situ* debenzylation was applied; the product **3** was obtained. An analogous procedure with methylamine did not afford **4**; during the alkylation a rupture of the γ-lactone ring occurred. However, the alkylation of methylamine with 6-bromo-6-deoxy-$O^3$-benzyl-L-ascorbic acid **6** was successful and *N*-methyl-6-amino-6-deoxy-$O^3$-benzyl-L-ascorbic acid **7** was obtained. After removal of the benzyl group by catalytic hydrogenation, product **4** was obtained.

6-Bromo-6-deoxy-$O^3$-benzyl-L-ascorbic acid **6** was prepared by stirring $O^2$,$O^3$-dibenzyl-$O^5$,$O^6$-isopropylidene-L-ascorbic acid [20] **8** at room temperature in HBr/HOAc solution, followed by a prolonged heating at 50°C in water bath. By heating **8** at 100°C in 50% HOAc, the isopropylidene group was removed [20]. The same effect was achieved by heating **8** in 48% HBr. However, in a nonaqueous medium two simultaneous reactions took place: addition of bromine at position C6 and monodebenzylation at position C2. The structural characterization of monobromo-monobenzyl-L-ascorbic acid **6** was based on spectral ($^1$H- and $^{13}$C-NMR) data, and the $O^3$ position of the benzyl group was confirmed by X-ray structure analysis (to be published).

*Solid-state conformation and X-ray structure analysis of 3*

The interatomic distances and bond angles of **3** are listed in table I. The values observed here are in general agreement with the values reviewed by Hvoslef [21, 22] and those in references [23] and [24]. The molecular structure with the atom numbering is shown in figure 1; the Ortep plot [25] is drawn with the thermal ellipsoids at the 50% probability level. Among the 15 structures of ascorbic acid and its derivatives found in Cambridge Structural Database, version 5.07 [26], **3** (our data) and **2** [24] are zwitterions in crystalline state. Dissociation at O3 was observed in all salts and in these two structures.

Since L-ascorbic acid **1** is a precursor of **3**, the 4*S* configuration is assumed. Therefore, the known chirality of C4 was used as an internal standard for the absolute configuration at C5; accordingly the absolute

**Table I.** Bond lengths (Å) and angles (°) of **3**.

| | | | |
|---|---|---|---|
| O(1) – C(1) | 1.234(3) | C(1) – O(4) – C(4) | 108.1(2) |
| O(2) – C(2) | 1.378(3) | C(6) – N(1) – C(7) | 112.7(2) |
| O(3) – C(3) | 1.274(3) | C(6) – N(1) – C(8) | 109.3(2) |
| O(4) – C(1) | 1.372(3) | C(7) – N(1) – C(8) | 110.4(2) |
| O(4) – C(4) | 1.447(3) | O(1) – C(1) – O(4) | 119.5(2) |
| O(5) – C(5) | 1.412(3) | O(1) – C(1) – C(2) | 129.8(2) |
| N(1) – C(6) | 1.496(3) | O(4) – C(1) – C(2) | 110.6(2) |
| N(1) – C(7) | 1.496(4) | O(2) – C(2) – C(1) | 123.4(2) |
| N(1) – C(8) | 1.492(3) | O(2) – C(2) – C(3) | 126.6(2) |
| C(1) – C(2) | 1.414(4) | C(1) – C(2) – C(3) | 109.9(2) |
| C(2) – C(3) | 1.368(4) | O(3) – C(3) – C(2) | 131.4(2) |
| C(3) – C(4) | 1.533(3) | O(3) – C(3) – C(4) | 122.4(2) |
| C(4) – C(5) | 1.522(4) | C(2) – C(3) – C(4) | 106.2(2) |
| C(5) – C(6) | 1.518(3) | O(4) – C(4) – C(3) | 105.0(2) |
| | | O(4) – C(4) – C(5) | 109.9(2) |
| | | C(3) – C(4) – C(5) | 113.1(2) |
| | | O(5) – C(5) – C(4) | 113.1(2) |
| | | O(5) – C(5) – C(6) | 106.3(2) |
| | | C(4) – C(5) – C(6) | 109.2(2) |
| | | N(1) – C(6) – C(5) | 112.4(2) |

configuration is 4*S*, 5*S*. The conformation in the solid states of **3** and of **1** [22] and **2** [24] are described by the torsion angles given in table II. The atom numbering is shown in chart 1 and figure 1. In the comparative table II, the signs of torsion angles are in agreement with the 4*S* absolute configuration, which is characteristic of L-ascorbic acid and its derivatives. The global molecular shape is mainly dictated by the conformation of a side chain (exocyclic bonds, table II). The

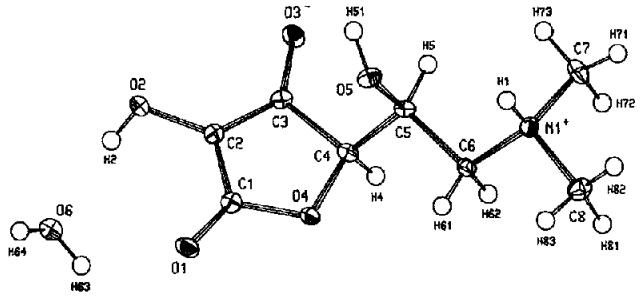


**Fig 1.** Ortep plot [25] with the atom numbering of **3**; the ellipsoids are scaled at the 50% probability level.

overall molecular conformations of **1** (**A** and **B**), **2** and **3** are shown in figure 2.

The position of C4-C5 bond results in (–)-anticlinal [27] conformation (for the atom sequence C2-C3-C4-C5) in **1** (A and B), **2** and **3**, which defines the orientation of a side chain towards the γ-lactone ring (~ –120°; table II). The conformation for the atom sequence C3-C4-C5-C6 (T1) is antiperiplanar (table II). This means that in the solid state the extended zig-zag shape of the aliphatic backbone is present (fig 2). In 6-amino-6-deoxy-substituted species, the conformation about C5-C6 is antiperiplanar as well (table II). However, both conformers of L-ascorbic acid reveal a (+)-synclinal conformation. The torsion angles involving O1, O2, and O3, due to the presence of C $sp^2$, are close to 180° (table II).

**Table II.** Torsion angles (°) of L-ascorbic acid and some of its 6-amino-6-deoxy-derivatives.

| | *1(A)** | *1(B)** | *2* | *3* |
|---|---|---|---|---|
| Endocyclic bonds | | | | |
| O4-C1-C2-C3 | –1.4(2) | 1.2(2) | 3.2(3) | –3.7(3) |
| C1-C2-C3-C4 | 1.3(2) | 2.4(2) | –1.1(3) | 2.7(3) |
| C2-C3-C4-O4 | –0.8(2) | –4.8(2) | –1.3(3) | –0.8(3) |
| C3-C4-O4-C1 | –0.1(5) | 5.4(2) | 3.2(2) | –1.4(3) |
| C4-O4-C1-C2 | 0.9(2) | –4.3(2) | –4.0(3) | 3.1(3) |
| Exocyclic bonds | | | | |
| C2-C3-C4-C5 | –121.8(4) | –125.2(4) | –123.1(2) | –120.7(2) |
| **C3-C4-C5-C6** | **–174.2(5)** | **172.2(5)** | **169.0(2)** | **178.1(2** |
| C3-C4-C5-O5 | 66.6(4) | 50.8(4) | 43.4(3) | 60.0(3) |
| **C4-C5-C6-O6** | **66.5(6)** | **64.8(7)** | – | – |
| **C4-C5-C6-N1** | – | – | **177.7(2)** | **174.5(2)** |
| C4-O4-C1-O1 | –177.7(2) | 176.7(2) | 176.1(2) | –177.1(2) |
| O4-C1-C2-O2 | –179.9(4) | –176.0(2) | 179.4(2) | 179.9(3) |
| C1-C2-C3-O3 | –179.0(2) | –177.7(2) | –179.9(3) | –176.4(3) |
| **C5-C6-N1-C7** | – | – | – | **–67.5(3)** |

*L-Ascorbic acid crystallizes with two conformers in the unit cell (**A** and **B**). Data for **1**(**A**), **1**(**B**), and **2** are from the references [22] and [24], respectively. The torsion angles given in bold define the conformation of a side chain.

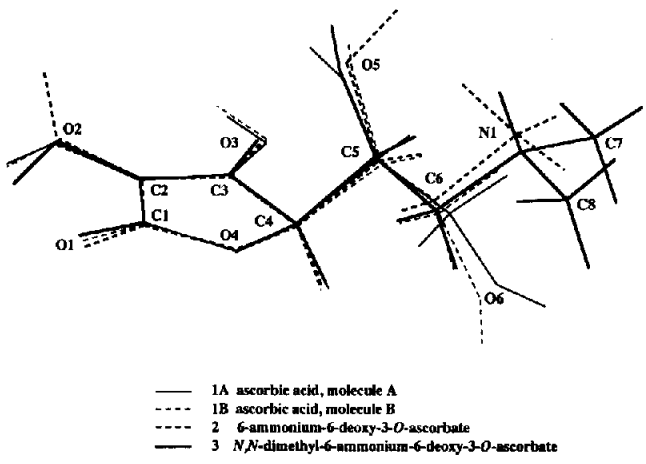


**Fig 2.** The superposition diagram of the molecular skeleton of **1**, **2** and **3** from the X-ray data; a fit was based on the best least-square planes of γ-lactone rings. The atomic coordinates of **1** and **2** were from references [22] and [24], respectively.

The conformation of γ-lactone ring is described by endocyclic torsion angles (table II), asymmetry parameters [28] and Cremer-Pople parameters [29, 30] listed in table III; the data reveal a departure from planarity towards envelope and twisted conformations. It is possible that hydrogen bonds influence the puckering of the γ-lactone ring. The crystal packing of **3** is dominated by a three-dimensional hydrogen bond network (table IV). The N-H group of dimethylammonium cation participates in the bifurcated hydrogen bonds between O5 (intramolecular) and O3 (intermolecular). Hydroxy group O2 is the proton donor to water oxygen atom (O6). Hydroxy group O5 is a donor to oxygen atom O1 of the lactone group. The crystalline water molecule contributes to the hydrogen bond network; it acts as the proton donor to hydroxy O2 and to deprotonated O3.

*Extended molecular modelling and comparative conformational analysis*

The conformational analysis of **1**, **2** and **3** was performed by semi-empirical methods (MNDO in MOPAC, version 6.0, Biosym, 1994) [31], molecular mechanics calculations and molecular dynamics simulations *in vacuo* using DISCOVER, version 2.95, based on cff91 force field (Biosym, 1994) [31]. The results were visualised using INSIGHT II, version 2.3.0 (Biosym, 1994) [31]. Molecular dynamics simulations were performed *in vacuo*, at 300K over 400 ps; simulations for **3** were also performed *in vacuo* at elevated temperatures (from 300 to 600K in 100K steps, 100 ps at each temperature) and in water at 300K over 400 ps. The starting geometry was from X-ray structure analysis (for **1** from reference [22], for **2** from reference [24], and for **3** from the present work). The calculations for **3** were carried out on the neutral molecule and zwitterion. The AMPAC/MOPAC [31] program was used to assign the partial charges to the zwitterion.

Conformational analysis was focused on a side chain in **3** and its comparison with corresponding side chains in **1** and **2** in order to select bioactive conformation(s). Three torsion angles are relevant for analysis: T1 = C3-C4-C5-C6, T2 = C4-C5-C6-R (R = O6, N1), and T3 = C5-C6-N1-C7 (table V). The results of the search of conformational space, summarized in table V, include optimized conformations. The occurrence of a particular conformational type, as a func-

**Table III.** Analysis of γ-lactone ring puckering in **1**, **2** and **3**.

| | *1(A)** | *1(B)** | *2* | *3* |
|---|---|---|---|---|
| Cremer-Pople ring puckering parameters [29, 30] | | | | |
| $q$ | 0.01 | 0.05 | 0.03 | 0.03 |
| φ(°) | 32.67 | 119.42 | 158.89 | 13.35 |
| Asymmetry parameters (°) [28, 48] | $\Delta C_s$(C2) = 0.1(2)<br>$\Delta C_2$(C1-C2) = 0.6(3) | $\Delta C_2$(C4-O4) = 0.9(2)<br>$\Delta C_s$(C4) = 1.4(2) | $\Delta C_2$(C1-O4) = 0.1(3) | $\Delta C_2$(C1-C2) = 0.5(3)<br>$\Delta C_s$(C1) = 1.0(3) |
| Weighted average absolute torsion angle (°) [48] | 1.1 | 3.7 | 2.7 | 2.3 |
| Conformation | $E_2/^1T_2$ | $^OT_4/E_4$ | $^OT_1$ | $^1T_2/^1E$ |

*L-Ascorbic acid crystallizes with two conformers in the unit cell (**A** and **B**). Data for **1(A)**, **1(B)**, and **2** are from the references [22] and [24], respectively.

**Table IV.** Hydrogen bonds in the crystal packing of **3**.

| | *D...A (Å)* | *D–H (Å)* | *H...A (Å)* | *D–H...A (°)* | *Symmetry operations on A* |
|---|---|---|---|---|---|
| N1-H1...O5 | 2.868(3) | 1.01(3) | 2.49(3) | 102(2) | *x, y, z* |
| N1-H1...O3 | 2.670(3) | 1.01(3) | 1.84(3) | 137(2) | $-x-1, 1/2+y-1, 1/2-z$ |
| O2-H2...O6* | 2.658(3) | 0.98(4) | 1.69(4) | 168(3) | *x, y, z* |
| O5-H51...O1 | 2.671(3) | 0.98(3) | 1.69(3) | 175(3) | $x-1, y, z$ |
| O6*-H63...O3 | 2.791(3) | 0.98(4) | 1.83(4) | 165(3) | $x+1, y, z$ |
| O6*-H64...O2 | 2.832(3) | 0.99(4) | 1.85(4) | 171(4) | $1/2+x, 1/2-y+1, -z$ |

*Water molecule.

tion of two torsion angles T1 and T2, is shown in figure 3a for **1**, figure 4a for **2** (the neutral molecule), figure 5a for the neutral molecule of **3** and figure 6a,b for the zwitterion of **3**. The variation of T3 in time (400 ps) for **3** is given in figures 5b and 6c (the neutral and zwitterion forms, respectively). The conformations recognized during molecular dynamics simulations for a given compound (**1**, **2** and **3**) are illustrated in the overlap diagrams (figs 3b, 4b, 5c and 6d).

The extended modelling of **3** included the neutral molecule and a zwitterion (observed in the crystal). Molecular mechanics calculations performed on **3** (for both forms) revealed antiperiplanar conformation about T1 and T2 (type **d**, table V) as in the crystal.

**Table V.** Comparative conformational analysis of a side chain based on X-ray data and extended computer modelling *in vacuo*.

| | *Conformational type* | *T1(°) C3-C4-C5-C6* | *T2(°) C4-C5-C6-R* | *T3(°) C5-C6-N1-C7* |
|---|---|---|---|---|
| *Compound 1* | | | *R = O6* | |
| X-ray, molecule **A** | **a** | –174.2(5) | 66.5(6) | – |
| X-ray, molecule **B** | **a** | 172.2(5) | 64.8(7) | – |
| Computer modelling, molecule **A** | | | | |
| MM | **a** | 173 | 59 | – |
| MD, 300K, 400 ps | **b** | 55 | 53 | – |
| | **c** | 60 | –65 | – |
| *Compound 2* | | | *R = N1* | |
| X-ray, zwitterion | **d** | 169.0(2) | 177.7(2) | – |
| Computer modelling, neutral molecule | | | | |
| MM | **d** | 173 | 176 | – |
| MD, 300K, 400 ps | **c** | 66 | –67 | – |
| *Compound 3* | | | *R = N1* | |
| X-ray, zwitterion | **d** | 178.1(2) | 174.5(2) | –67.5(3) |
| Computer modelling, neutral molecule | | | | |
| MM | **d** | 175 | 169 | –64 |
| MD, 300K, 400 ps | $\mathbf{a_1}$ | 173 | 55 | –166 |
| | $\mathbf{a_2}$ | –176 | 54 | 63 |
| | **d** | –179 | 177 | –65 |
| Computer modelling, zwitterion | | | | |
| MM | **d** | 170 | –164 | –64 |
| MD, 300K, 400 ps | **c** | 57 | –59 | –76 |
| MD, 500 and 600K | **b** | 42 | 41 | –158 |

Abbreviations: MM = molecular mechanics calculations; MD = molecular dynamics simulations. Conformation types (the angle ranges are given according to Klyne and Prelog [27]): **a**) T1 ~ ±180°, T2 ~ 60° (extended); **b**) T1 ~ 60°, T2 ~ 60° (folded); **c**) T1 ~ 60°, T2 ~ –60° (folded); and **d**) T1 ~ ±180°, T2 ~ ±180° (extended).

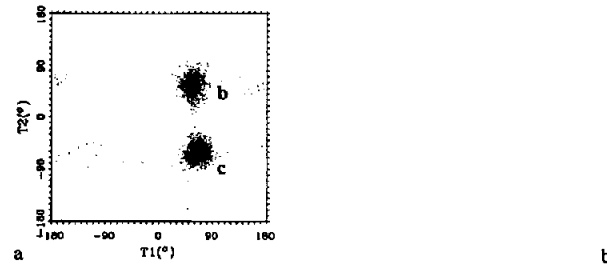


**Fig 3.** (**a**) The occurrence of two conformations (type **b** and type **c**) of **1** during MD at 300K over 400 ps defined with torsion angles T1 and T2; (**b**) the overlap diagram of MM and X-ray extended conformation (type **a**) and two folded conformations by MD (types **b** and **c**).

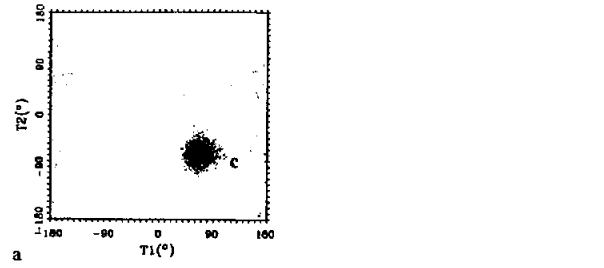


**Fig 4.** (**a**) The occurrence of the conformation type **c** of **2** (the neutral molecule) during MD at 300K over 400 ps defined by the torsion angles T1 and T2; (**b**) the overlap diagram of the conformations recognized by MM and X-ray (type **d**) and MD (type **c**).

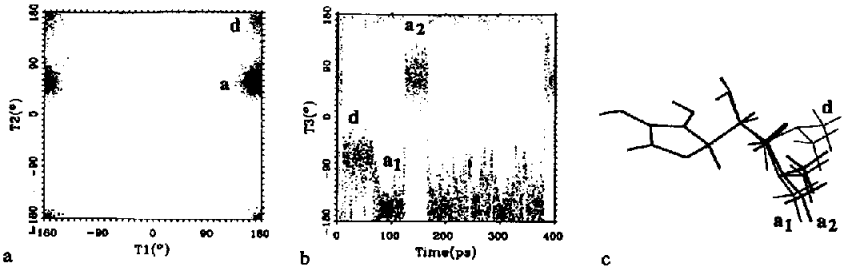


**Fig 5.** (**a**) The occurrence of the particular conformations (types **a** and **d**) of **3** (the neutral molecule) during MD at 300K over 400 ps shown as a function of torsion angles T1 and T2; (**b**) the variations of torsion angle T3 with time; (**c**) the overlap diagram of the extended conformations from MM and X ray (type **d**) and from MD (types $\mathbf{a}_1$, $\mathbf{a}_2$ and **d**).

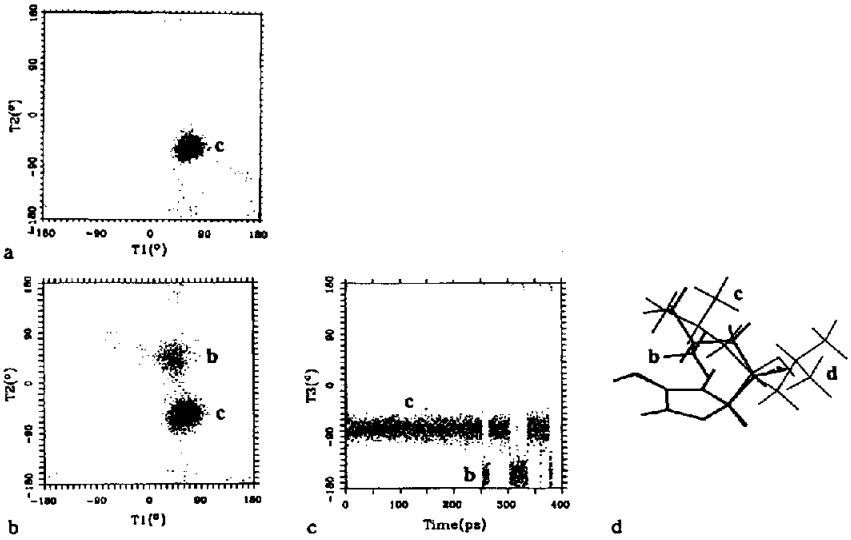


**Fig 6.** The occurrence of the particular conformations of **3** (a zwitterion) during MD as a function of torsion angles T1 and T2 at: (**a**) 300 K over 400 ps and (**b**) 300–600K over 400 ps; (**c**) the variations of torsion angle T3 with time at 300–600K; (**d**) the overlap diagram of conformations detected in MM and X-ray (type **d**) and MD (types **b** and **c**).

Molecular dynamics simulations *in vacuo*, at 300K over 400 ps, detected an antiperiplanar conformation about T1 for the neutral molecule (fig 5a) whereas in the zwitterion a (+)-synclinal conformation was observed (figs 6a and 6b). About T2 (+)-synclinal and antiperiplanar conformations were observed in the neutral molecule (fig 5a) whereas in the zwitterion at 300K (–)-synclinal conformation was detected (fig 6a) and the (+)-synclinal conformation at elevated temperatures (at 500 and 600K) (fig 6b). For the neutral molecule of **3** those values for T1 and T2 define extended conformations of the types **a** and **d** (table V, fig 5c). For the zwitterion of **3**, folded conformations dominate (types **b** and **c**, table V, fig 6d). The values of T3 (C5-C6-N1-$CH_3$) describe the orientation of the terminal part of a side chain. Both methyl groups are sterically equivalent and for the conformational analysis, one of them is arbitrarily selected (C7, table V). During the conformational search for energy optimal conformation(s), three distinctive conformations about C6-N1 (T3) were observed: antiperiplanar, (+)-synclinal and (–)-synclinal (table V). These types were seen in the neutral molecule (fig 5b), whereas (–)-synclinal and antiperiplanar (at 500 and 600K) conformations appeared in the zwitterion (table V, fig 6c). The values of T1 and T2 are relevant for the overall molecular conformation; for **3** it is characterized by four different families of conformations. Two of them correspond to the extended side chain (T1 ~ ±180°, T2 ~ 60° (type **a**); T1 ~ T2 ~ ±180° (type **d**)) (fig 5c) and the other two (T1 ~ T2 ~ 60° (type **b**); T1 ~ 60°, T2 ~ –60° (type **c**)) to the folded one (fig 6d). Thus, for the zwitterion of **3** the extended conformation (type **d**) was observed in the solid state, whereas *in vacuo* modelling revealed folded conformations of types **b** and **c**. The molecular mechanics DRIVE option performed for T1 and T2 of the zwitterion of **3** also revealed the energy minima conformers of the types **b** (for T3 = –158°) and **c** (for T3 = –76°).

For comparison with **3**, the conformational analyses of **1** and **2** are given (table V).

In the molecule of L-ascorbic acid **1**, molecular mechanics calculations revealed optimal conformations about T1 and T2 as in the crystal [22] (antiperiplanar for T1 and (±)-synclinal for T2, type **a**, table V). However, molecular dynamics simulations at 300K over 400 ps showed (+)-synclinal conformation about T1 and (+)-synclinal about T2 (types **b** and **c**, table V, figs 3a and 3b). Intramolecular hydrogen bonds O2-H...O1 and O3-H...O2 were observed in extended and folded conformations recognized during molecular mechanics and molecular dynamics simulations *in vacuo* (table V). According to an *ab initio* study [32] of ascorbic acid (in the gas phase) with the STO-3G optimization, nine different staggered conformers were located with the largest energy difference between the nine local minima of 5.1 kcal $mol^{-1}$. All of them were stabilized by the intramolecular hydrogen bonds. These results are in agreement with our findings.

In our study two distinctive conformations of **2** were observed. Molecular mechanics calculations revealed the antiperiplanar conformation about T1 and T2 (table V) as in **3**. This conformation corresponds to the extended form (type **d**) (fig 4b), which was also detected in the zwitterion in the solid state. Molecular dynamics simulations at 300K gave (+)-synclinal conformation about T1 and (–)-synclinal conformation about T2 (table V, fig 4a) which define the folded conformation of type **c** (fig 4b).

The extended conformations are in favour of intermolecular hydrogen bonds. In the polar environment, as in the crystal and in water, these interactions are present; preliminary molecular dynamics simulations in water for the zwitterion of **3** revealed extended conformation of the type **d**. However, in nondisturbed environment, *eg*, *in vacuo*, the folded conformations are preferred. They are stabilized with intramolecular hydrogen bonds. The substitution at C6 with amino or dimethylamino groups makes molecules adopt the zwitterion form with the formation of an ammonium cation which favours N-H...O5 or N-H...O3 intra- or intermolecular hydrogen bonds; the orientation of the proton dictates the formation of particular hydrogen bonds.

*Cytotoxic activity of 3*

There is some experimental evidence [2, 3] that ascorbic acid may directly inhibit the growth of proliferating cells. The extent of inhibition depends on the amount of ascorbate absorbed by a given cell and on the sensitivity of the cell to its cytotoxic effect. Synthesis of new amino derivatives of ascorbic acid and their screening for cytotoxic activity, have shown that such modifications enhance the cytotoxic activity of the parent compound (ascorbic acid **1**). The strongest inhibition of the growth of HeLa cells was achieved with **2** [33] and **3**. Some inhibition was achieved with **4** (results are not shown). In the present study, the influence of *N,N*-dimethyl-6-amino-6-deoxy-L-ascorbic acid **3** was examined in relation to the parent compound **1**, on the growth of fibroblasts (WI 38) and three human tumour cell lines (Hep2, MiaPaCa2 and HeLa).

The inhibitory effect of **1** and **3** on various cultured cell lines is presented in figures 7a and 7b, respectively. All cell lines were incubated with different concentrations of **1** and **3** for 3 d. The most pronounced inhibitory effect was obtained with the highest concentrations used (2 and 3 mM). The substances were used at relatively high concentra-

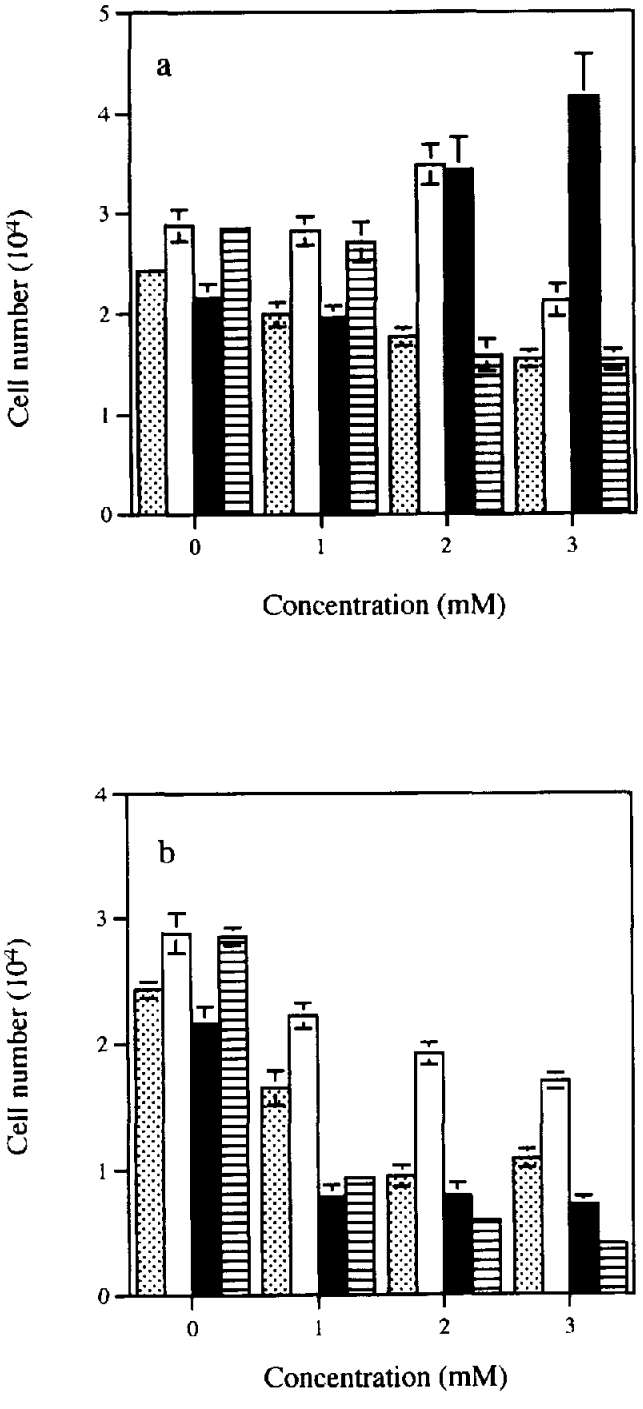


**Fig 7.** Inhibitory effect of different concentrations of ascorbic acid **1** (**a**) and dimethylaminoascorbic acid **3** (**b**) on the growth of WI 38 (dotted column), Hep2 (white column), MiaPaCa2 (black column) and HeLa (striped column) cells measured after 72 h of exposure. Each column represents the mean ± SD ($n = 4$).

tions, but a similar effect with **1** was also achieved by other authors [2, 34].

The growth inhibitory effect of **1** and **3** varied from one type of cells to the other. The compound **1** did not inhibit the growth of Hep2 and MiaPaCa2 cell lines, while it inhibited the growth of WI 38 (20–40%) and HeLa cells (50%) at high concentrations (fig 7a). However, **3** exhibited a strong cytotoxic effect on all examined cell lines, being the least pronounced on Hep2, and the strongest on HeLa cells (fig 7b). The results indicate that the substitution on the C6 atom of **1** improved cytotoxic activity in comparison with the parent compound. A similar observation was made earlier with 6-bromo-6-deoxy-L-ascorbic acid [4].

To find out the possible mechanism of cell death after treatment with **3**, the expression of two genes involved in cell proliferation and death (*c-myc* and *p53*) has been investigated. The expression of the *c-myc* gene leads to cell proliferation, but under certain circumstances its overexpression could also induce apoptosis [35, 36]. Mutation of the *p53* gene and accumulation of its aberrant protein are the most common alterations detected in many types of human cancers [37, 38]. The compound **3** might cause changes in *c-myc* and *p53* mutated gene expression and affect the growth of tumour cells.

Using immunocytochemical methods, the expression of c-Myc oncoprotein and *p53* mutated protein was examined on Hep2, WI 38, MiaPaCa2 and HeLa cell lines with and without addition of 2 mM solution of **3** for 24 h. The slides were analysed using a light microscope and image analyser. The results obtained by these analyses did not indicate a significant difference in the expression of these genes between the control and treated cells, not even in HeLa cells where **3** caused the strongest growth inhibition and drastic morphological changes (figs 8c and 8d). The only difference seen was the localization of these two proteins. In the control cells (figs 8a and 8b), they were located in the nucleus, but after treatment of the cells with **3** they also appeared in the cytoplasm. This might have been due to nuclear membrane damage.

Light microscopy of the cells incubated with 2 mM solution of **3** showed significant morphological changes, such as a round shape, smaller volume, chromatin condensation and nuclear fragmentation. These changes are characteristic of cells undergoing apoptosis [39, 40]. The appearance of the morphological features of apoptosis was the most prominent on HeLa cells (figs 8c and 8d). Apoptosis is also characterized by activation of endonucleases that cut DNA between nucleosomes, giving rise to a 'ladder' of nucleosomal-sized multimers [41, 42].

To investigate whether the cell death induced by **3** was associated with apoptosis, DNA fragmentation was examined. The results obtained by agarose gel

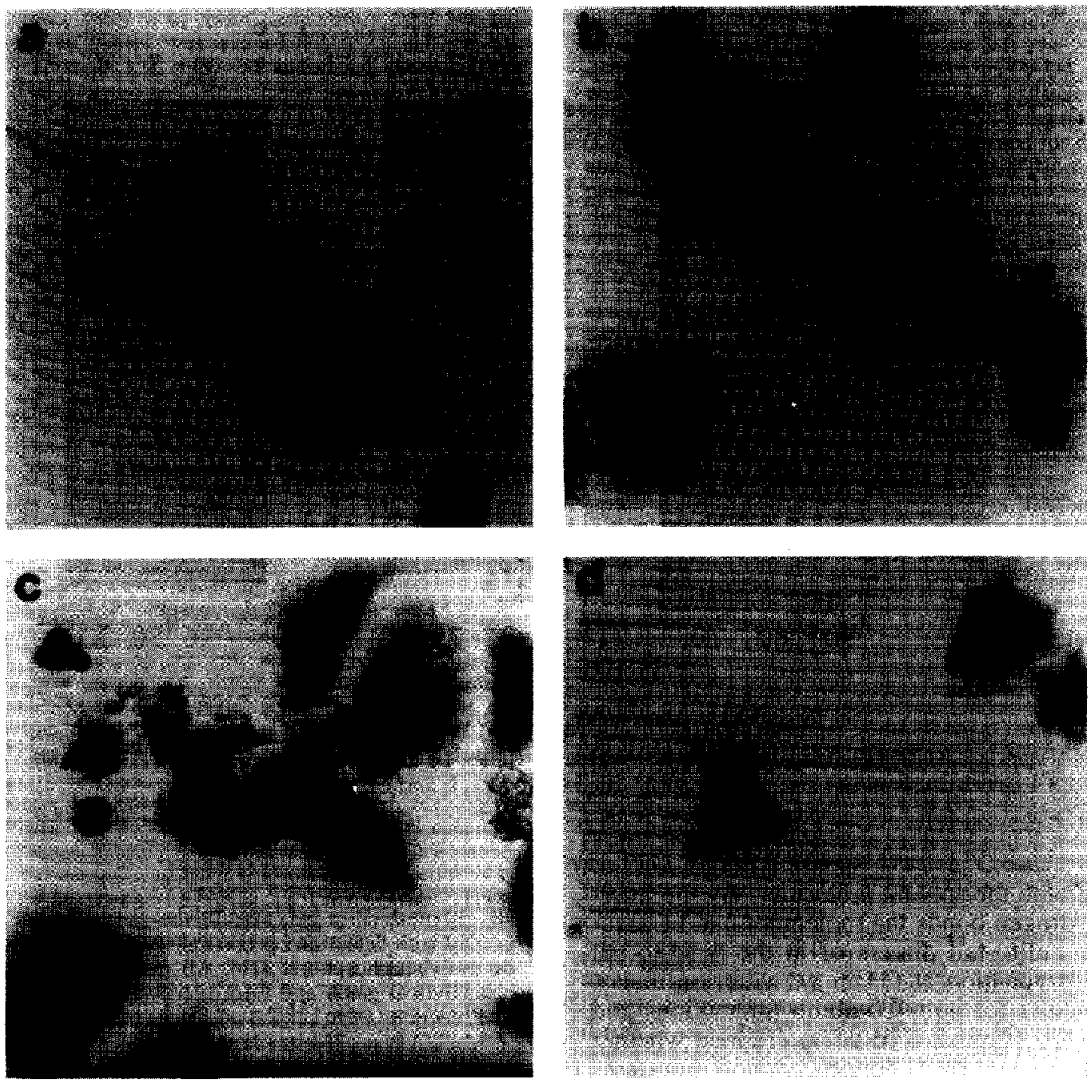

**Fig 8.** Immunocytochemical staining of *c-Myc* (**a** and **c**) and *p53* (**b** and **d**) gene products in HeLa cells. Control cells (**a** and **b**) and cells after 24 h of exposure to 2 mM dimethylaminoascorbic acid **3** (**c** and **d**).

electrophoresis (fig 9, lanes a4, b4 and c4) show the presence of DNA fragmentation. The extent of DNA fragmentation differed from one cell type to another and it was in correlation with the growth inhibition (fig 7), morphological changes (fig 8) and cell viability (fig 9).

## Conclusion

The substitution at C6 of L-ascorbic acid with amino [33] and alkylated amino groups (this work) produces compounds with cytotoxic activity. *N,N*-Dimethyl-6-amino-6-deoxy-L-ascorbic acid **3** enhances cytotoxic activity *in vitro*. Since characteristic morphological changes and ladder DNA fragmentation was observed, cells treated with **3** probably died by apoptosis, although the other mechanisms of cell death are not excluded. Apoptosis was not mediated by c-myc or p53 proteins, since **3** did not significantly influence their expression.

The molecule of **3** appears as a zwitterion in the polar media, *eg*, in the crystal and polar solvents, and probably at physiological pH as well. The ammonium cation at the tail of the molecule is available as a donor for intermolecular hydrogen bonds with other

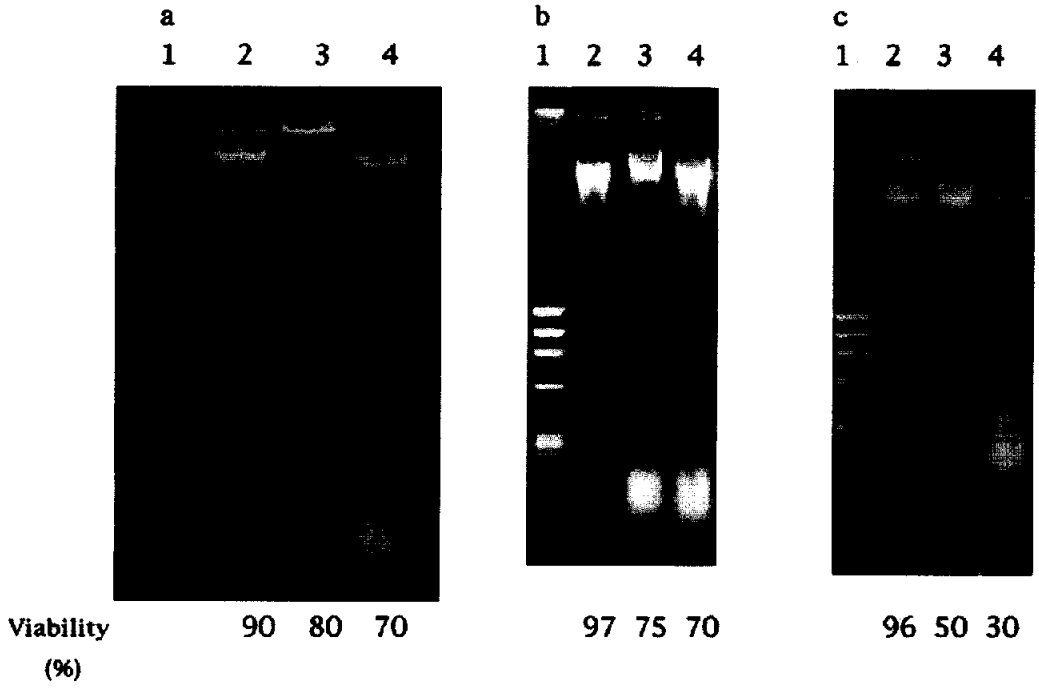


**Fig 9.** Agarose gel electrophoresis of DNA isolated from Hep2 (**a**), WI 38 (**b**) and HeLa (**c**) cells, and corresponding cell viabilities. DNA standard λ/HindIII (lane **1a**) and ϕ x 174/Hae III (lanes **1b** and **c**), DNA from control cells (lanes **2a, b** and **c**), cells treated with **1** (lanes **3a, b** and **c**) and cells treated with **3** (lanes **4a, b** and **c**).

molecules or with the solvent molecules. By the intermolecular hydrogen bonds the molecules can be associated in the tail-to-tail dimers or in the head-to-tail polymer. Deprotonation at O3 in a zwitterion makes this site available for both Coulomb interactions and hydrogen bonds. It remains to be ascertained whether the formation of hydrogen-bonded adducts interferes with the usual cell mechanisms or whether this polar molecule disturbs certain gate mechanisms. The lack of knowledge about the ascorbate mechanisms *in vivo* prevents us from proposing their mode of action at the molecular level in pathological conditions.

## Experimental protocols

*Synthesis*

Melting points are uncorrected. IR spectra were recorded using a Perkin Elmer FTIE 1725 X spectrometer. Mass spectra (EI, 70 eV) were recorded by an Extrel FTMS 2001 DD spectrometer and $^1$H- and $^{13}$C-NMR were obtained using a Varian Gemini 300 spectrometer at 300 and 75 MHz, respectively. Chemical shifts were reported in ppm units with TMS as the internal standard. Coupling constants were reported in hertz. Microanalyses were performed with a Perkin Elmer 2400 analyzer. Silica-gel 60 $F_{254}$ plates (Merck) were used for TLC; 70-230 mesh silica gel (Merck) was used for column chromatography with detection by UV light at 254 nm or by 5% alcoholic molybdophosphoric acid. All chemicals and solvents were of analytical grade and were used without further purification. The reactions were carried out under nitrogen where necessary.

*N,N-Dimethyl-6-amino-6-deoxy-L-ascorbic acid 3*

*Method A.* To a solution of 6-amino-6-deoxy-L-ascorbic acid [43] **2** (2.2 g, 12.5 mmol) in water (150 mL) 37% aqueous formaldehyde (9.4 mL, 125 mmol), sodium cyanoborohydride (2.3 g, 36.5 mmol) and glacial acetic acid (1.2 mL) were added and the reaction mixture was stirred at room temperature for 4 h, under a nitrogen atmosphere. Removal of the solvent gave crude material which was chromatographed on a column of silica gel with mixture of methanol/water (7:3) to give **3** as a white solid (0.88 g, 35%): mp 208–210°C (dec); IR (KBr) 3400, 1750, 1650, 1480, 1100, 1050, 950 cm$^{-1}$; $^1$H-NMR ($D_2O$) δ 2.83 (s, 6H, $N(CH_3)_2$), 3.22–3.38 (m, 2H, $C^6$-$H_2$), 4.20–4.26 (m, 1H, $C^5$-H), 4.285 (d, 1H, $J$ = 2.2, $C^4$-H); $^{13}$C-NMR ($D_2O$) δ 43.97 ($N(CH_3)_2$), 60.17 (C-6), 64.80 (C-5), 79.39 (C-4), 114.15 (C-2), 174.84 (C-3), 177.87 (C-1); MS (*m/z*) (203 M$^+$); Anal $C_8H_{13}NO_5$ (C, H, N).

*Method B.* To a solution of 6-bromo-6-deoxy-$O^2$,$O^3$-dibenzyl-L-ascorbic acid [19] **5** (1 g, 2.4 mmol) in methanol (10 mL) was added a methanolic solution of dimethylamine (20%, 5 mL). The reaction mixture was stirred in an atmo-

sphere of nitrogen, for 3 h at room temperature, and left to stand overnight. Methanol was evaporated to a volume of 10 mL, then 10% Pd/C (35 mg) was added and the reaction mixture was hydrogenated in a Parr shaker apparatus at 2 bar hydrogen pressure for 3 h. The catalyst was removed by filtration and the filtrate was evaporated. The residue was purified by chromatography on silica gel (methanol/water: 7:3) to give **3** (0.1 g, 20%).

*N-Methyl-6-amino-6-deoxy-L-ascorbic acid* **4**

To a solution of *N*-methyl-6-amino-6-deoxy-$O^3$-benzyl-L-ascorbic acid **7** (1.4 g, 5 mmol) in methanol (150 mL), 10% Pd/C (150 mg) was added and the reaction mixture was hydrogenated in a Parr shaker apparatus at 2 bar hydrogen pressure for 3 h. The catalyst was removed by filtration, the filtrate was evaporated and the residue was purified by column chromatography (silica gel, methanol/water: 7:3) to afford **4** as a yellow solid (0.2 g, 21%): mp 158–160°C; IR (KBr) 3400, 1740, 1600, 1380, 1150, 1050 $cm^{-1}$; $^1$H-NMR ($D_2O$) δ 2.73 (s, 3H, $CH_3$), 3.26–3.30 (dd, 2H, $J_1$ = 3.5, $J_2$ = 9.1, $C^6$-$H_2$), 4.20–4.25 (m, 1H, $C^5$-H), 4.415 (d, 1H, $J$ = 1.8, $C^4$-H); $^{13}$C-NMR ($D_2O$) δ 33.91 ($CH_3$), 52.18 (C-6), 65.68 (C-5), 79.22 (C-4), 115.22 (C-2), 170.53 (C-3), 176.96 (C-1); Anal $C_7H_{11}NO_5$ (C, H, N).

*6-Bromo-6-deoxy-$O^3$-benzyl-L-ascorbic acid* **6**

To $O^2$,$O^3$-dibenzyl-$O^5$,$O^6$-isopropyliden-L-ascorbic acid [20] **8** (1 g, 2.5 mmol) was added hydrobromic acid (33% in acetic acid, 15 mL). The reaction mixture was stirred for 1.5 h at room temperature. Afterwards, water (100 mL) was added and the solution was heated at 50°C for 25 h. The excess of HBr gas was removed by a stream of nitrogen gas at 50°C for 2 h. The solvent was evaporated to half volume and the solution was extracted with methylene chloride (50 mL). The organic phase was separated, dried and evaporated, leaving a yellow oily residue which was purified on a silica-gel column (methylene chloride/ethanol: 95:5) to give **6** (0.4 g, 48%) as a semisolid that was crystallized from chloroform to afford **6** as a white crystalline solid: mp 88–90°C; IR (neat) 3400, 1760, 1690, 1330, 1150 $cm^{-1}$; $^1$H-NMR ($CD_3OD$) δ 3.44–3.50 (dd, 1H, $J_1$ = 7.1, $J_2$ = 10.3, $C^6$-H), 3.53–3.59 (dd, 1H, $J_1$ = 6.8, $J_2$ = 10.3, $C^6$-H), 3.98–4.03 (m, 1H, $C^5$-H), 4.89 (d, 1H, $J$ = 1.9, $C^4$-H); $^{13}$C-NMR ($CD_3OD$) δ 33.55 (C-6), 70.80 (C-5), 74.40 ($CH_2Ph$), 77.50 (C-4), 121.78 (C-2), 129.51–129.98 (CH-Ph), 138.20 (C-Ph), 151.64 (C-3), 173.03 (C-1); MS (*m/z*) (329 $M^+$) (328 $M^+$ – 1); Anal $C_{13}H_{13}BrO_5$ (C, H, Br).

*N-Methyl-6-amino-6-deoxy-$O^3$-benzyl-L-ascorbic acid* **7**

To a solution of 6-bromo-6-deoxy-$O^3$-benzyl-L-ascorbic acid **6** (1 g, 3 mmol) in methanol (20 mL), a methanolic solution of methylamine (20%, 5 mL) was added. The reaction mixture was stirred for 3 h under a nitrogen atmosphere and was kept at room temperature overnight. Evaporation of the solvent and chromatographic purification of the residue (silica gel, methylene chloride/methanol: 7:3) furnished **7** (0.43 g, 51%) as an oily product: IR (neat) 3400, 1650, 1500, 1420, 1250, 900 $cm^{-1}$; $^1$H-NMR ($CD_3OD$) δ 2.72 (s, 3H, $CH_3$), 3.14–3.27 (m, 2H, $C^6$-$H_2$), 4.18–4.23 (m, 1H, $C^5$-H), 4.745 (d, 1H, $J$ = 2.1, $C^4$-H), 5.47–5.63 (2d, 2H, $J$ = 11.7, $OCH_2Ph$), 7.33–7.49 (m, 5H, Ph-H); $^{13}$C-NMR ($CD_3OD$) δ 33.98 ($CH_3$), 52.52 (C-6), 65.86 (C-5), 74.18 ($CH_2Ph$), 77.85 (C-4), 121.95 (C-2), 128.97–129.78 (CH-Ph), 137.80 (C-Ph), 150.38 (C-3), 172.39 (C-1); Anal $C_{14}H_{17}NO_5$ (C, H, N).

*X-ray structure determination of* **3**

Crystals suitable for X-ray analysis were grown from water solution by the liquid diffusion method using *n*-propanol as precipitant at 4°C for 8 d. The crystal data and summary of the experimental details are listed in table VI. The X-ray intensity data were collected with an Enraf-Nonius CAD4 diffractometer with graphite-monochromatized Cu*K*α radiation. According to the variations in intensities of standard reflections, a decay of 0.4% was detected. The data were corrected for decay, Lorentz and polarization effects, using the Enraf-Nonius SDP/VAX package [44]. The structure was solved by SHELX86 [45]. Refinement was by full-matrix least-squares method minimizing $\Sigma\,(|F_o| - |F_c|)^2$ with the SHELX76 [46] system of programs using $F$ values. Atomic scattering factors were those included in SHELX76 [46]. Details of the refinement procedures are given in table VI and final atomic coordinates in table VII. During structure determination, the L-enantiomer was selected according to the assignment *S* at C4; chirality on C5 proved to be *S*. The molecular geometry was calculated by the PLUTON program incorporated in EUCLID [47], OrtepII [25] and Barbara [48]. The O-H and N-H distances were normalized to the values obtained by neutron diffraction (O-H 0.983 Å, N-H 1.009 Å) [49].

All calculations were performed on IRIS-4D25G work station of the X-ray Laboratory, Rudjer Bošković Institute (Zagreb, Croatia).

Final atomic parameters for *N,N*-dimethyl-6-amino-6-deoxy-L-ascorbic acid **3** have been deposited at the Crystallographic Data Centre, Cambridge, UK.

*Biology*

*Materials for biological tests*

Dulbecco's Modified Eagle Medium (DMEM), fetal calf serum (FCS) and ϕ x 174 RF DNA/Hae III molecular weight marker were purchased from GIBCO (Grand Island, NY). L-Ascorbic acid **1**, *N,N*-dimethyl-6-amino-6-deoxy-L-ascorbic acid **3** and *N*-methyl-6 amino-6-deoxy-L-ascorbic acid **4** were prepared in the Pliva Research Institute (Zagreb, Croatia). RNase A and proteinase K were purchased from Sigma. All other chemicals were of analytical grade.

*Cell culturing*

Human cell lines WI 38 (diploid fibroblasts), MiaPaCa2 (pancreatic carcinoma), Hep2 (laryngeal carcinoma) and HeLa (cervical carcinoma) were cultured in DMEM supplemented with 10% fetal calf serum, 2 mM glutamine, 100 U/mL penicillin and 100 mg/mL streptomycin in a humidified atmosphere with 5% $CO_2$ at 37°C. The cells were plated at a concentration of 1 x $10^4$ cells/mL onto 24-microwell plates. Following overnight incubation at 37°C, **3** was added at concentrations of 1, 2 and 3 mM. Control cells were grown under the same conditions without addition of **3**. Three days after plating, the cells were counted in an electronic counter (Model ZM, Coulter Electronics Ltd, UK). The number of control and treated cells represent means of four parallel samples. Cell viability was assessed by trypan blue exclusion.

*DNA isolation and electrophoresis*

DNA from control and treated cells was isolated according to the procedure described by Sambrook *et al* [50]. After washing with phosphate-buffered saline, the cells were resuspended in Tris/EDTA buffer and lysed in lysis buffer (50 mM Tris-Cl, pH 8, 10 mM EDTA, 0.5% w/v sodium dodecyl sulphate (SDS), 20 mg/mL RNase) for 1 h at 37°C. Proteinase K (100 mg/mL) was then added to the mixture and left to stand for 3 h at 50°C. DNA was extracted with phenol/chloroform. The isolated DNA (5 μg) was analyzed by agarose (1.5%) gel electrophoresis.

**Table VI.** Summary of crystal data and details of structure determination of **3**.

| | |
|---|---|
| **a) Crystal data** | |
| Molecular formula | $C_8H_{13}NO_5 \times H_2O$ |
| $M_r$ | 221.2 |
| Crystal size (mm) | 0.60 x 0.25 x 0.06 |
| $a$ (Å) | 5.853(1) |
| $b$ (Å) | 8.490(4) |
| $c$ (Å) | 19.873(5) |
| $V$ (Å$^3$) | 987.6(6) |
| Crystal system | orthorhombic |
| Space group | $P2_12_12_1$ |
| $Z$ | 4 |
| $D_{calc}$ (gcm$^{-3}$) | 1.488 |
| $\mu$ (cm$^{-1}$) | 1.2 |
| $F_{000}$ (electrons) | 472 |
| **b) Data collection** | |
| Diffractometer | Enraf-Nonius CAD-4 |
| Radiation | Mo$K\alpha$ |
| $\lambda$ (Å) | 0.71073 |
| T (K) | 105(3) |
| No of reflections used for cell parameters | 25 |
| $\theta$ range (°) | 6–18 |
| $\theta$ range for intensity measurement (°) | 2–28 |
| *hkl* range | –1, 7; –1, 11; –1, 26 |
| scan | $\omega/\Theta$ |
| No of measured reflections | 2237 |
| No of symmetrical independent reflections | 1316, $I > 2\sigma(I)$ |
| **c) Refinement** | |
| No of variables | 196 |
| Quantity minimised | $\Sigma w(\lvert F_o\rvert - \lvert F_c\rvert)^2$; $w = 1.8515 / [\sigma^2(F) + 0.000283\,(F^2)]$ |
| $R, R_w$, S | 0.035, 0.034, 0.59 |
| Final <shift / error> | 0.001 |
| Residual electron density $(\Delta\rho)_{max}$, $(\Delta\rho)_{min}$ (eÅ$^{-3}$) | 0.43, –0.32 |

**Table VII.** Final atomic coordinates and equivalent isotropic thermal parameters of the non-hydrogen atoms for **3**.

| *Atom* | *x* | *y* | *z* | $U_{eq}$(Å$^2$) |
|---|---|---|---|---|
| O(1) | 0.3193(3) | 0.7524(2) | 0.1444(1) | 0.0153(5) |
| O(2) | 0.0156(3) | 0.8830(3) | 0.0385(1) | 0.0145(6) |
| O(3) | –0.3465(3) | 1.0571(2) | 0.1187(1) | 0.0145(5) |
| O(4) | 0.0947(3) | 0.8809(2) | 0.2183(1) | 0.0126(5) |
| O(5) | –0.3456(3) | 0.7392(2) | 0.2354(1) | 0.0139(5) |
| N(1) | –0.4077(4) | 0.8216(3) | 0.3742(1) | 0.0111(6) |
| C(1) | 0.1522(5) | 0.8382(3) | 0.1539(1) | 0.0118(7) |
| C(2) | –0.0010(5) | 0.9056(3) | 0.1070(1) | 0.0113(7) |
| C(3) | –0.1697(5) | 0.9856(3) | 0.1402(1) | 0.0111(7) |
| C(4) | –0.1122(5) | 0.9739(3) | 0.2153(1) | 0.0110(7) |
| C(5) | –0.2993(5) | 0.8949(3) | 0.2564(1) | 0.0106(7) |
| C(6) | –0.2236(5) | 0.8840(3) | 0.3293(1) | 0.0110(7) |
| C(7) | –0.6049(5) | 0.9326(3) | 0.3809(2) | 0.0164(8) |
| C(8) | –0.3093(6) | 0.7851(3) | 0.4417(1) | 0.0155(8) |
| O(6)* | 0.4481(4) | 0.9323(2) | 0.0037(1) | 0.0164(6) |

$U_{eq} = (1/3)\,\Sigma_i\,\Sigma_j\,U_{ij}\,a_i^*\,a_j^*\,a_i \cdot a_j$. *Water molecule.

*Immunocytochemical detection of oncoproteins*
Immunocytochemical detection of *c-myc* and *p53* gene products was performed as described previously [51]. Mouse monoclonal antibody 155-11c7 to c-myc (Microbiological Associated, Bethesda, MD), mouse monoclonal IgG1 (Ab-3) to human mutant p53 (Oncogene Science, Manhasset, NY) and peroxidase-anti-peroxidase conjugate (PAP, DAKOPATTS) were used. The slides were stained with 0.025% diaminobenzidine tetrahydrochloride (DAB, Sigma) and analysed by light microscopy and an SAS-M image analyser [52].

## Acknowledgments

This work was supported partially by the Ministry of Science and Technology of the Republic of Croatia, Grants No. 1-08-144, 1-07-179 and 1-07-035. We express our gratitude to T Wein, application scientist from Biosym Technologies, München, for discussing the calculation strategy for charged molecules with one of authors (B Kojić-Prodić).

## References

1 Peterkofsky B, Prather W (1976) *J Cell Physiol* 90, 61–70
2 Bram S, Froussard P, Guichard M *et al* (1980) *Nature (Lond)* 284, 629–631
3 Pavelić K, Kos Z, Spaventi Š (1989) *Int J Biochem* 21, 931–935
4 Osmak M, Eckert-Maksić M, Pavelić K *et al* (1990) *Res Exp Med* 190, 443–449
5 Bowman RE, Stroud HH (1950) *J Chem Soc* 1342–1349
6 Borch RF, Hassid AI (1972) *J Org Chem* 37, 1673–1674
7 Sondengam BL, Hémo JH, Charles G (1973) *Tetrahedron Lett* 3, 261–263
8 Boldrini GP, Panunzio M, Umanironchi A (1974) *Synthesis* 733–735
9 Giumanini AG, Chiavari G, Musiani MM, Rossi P (1980) *Synthesis* 743–746
10 Loibner H, Pruckner A, Stütz A (1984) *Tetrahedron Lett* 25, 2535–2536
11 Kim S, Ho Oh C, Suk Ko J, Han Ahn K, Jin Kim Y (1985) *J Org Chem* 50, 1927–1932
12 Watanabe Y, Chul Shim S, Mitsudo T (1976) *Bull Chem Soc Jpn* 49, 1378–1380
13 Bhattacharyya S, Chatterjee A, Duttachowdhury S (1994) *J Chem Soc Perkin Trans* 1, 1–2
14 Verardo G, Giumanini AG, Strazzolini P (1994) *Synth Commun* 24, 609–627
15 Horner JK, Skinner WA (1966) *Can J Chem* 44, 315–319
16 Kadin SB (1973) *J Org Chem* 38, 1348–1350
17 Crochet RA, Blanton CDW (1974) *Synthesis* 55–56
18 Briggs EM, Brown GW, Jiricny J, Meidine MF ( 1980) *Synthesis* 295–296
19 Dallacker VF, Sanders J (1985) *Chem Ztg* 109, 277–280
20 Dallacker VF, Sanders J (1985) *Chem Ztg* 109, 197–202
21 Hvoslef J (1982) *In: Ascorbic Acid: Chemistry, Metabolism, and Uses, Advances in Chemistry*, Series 200, Am Chem Soc, Washington DC, 37–57
22 Hvoslef J (1968) *Acta Cryst* B24, 23–35
23 Ružić-Toroš, Ž Kojić-Prodić B, Horvatić D (1989) *Acta Cryst* C45, 269–273
24 Kojić-Prodić B, Danilović Ž, Puntarec V, Tomić S (1991) *Croat Chem Acta* 64, 311–317
25 Johnson CK (1976) *ORTEP II, Report ORLN-5138*. Oak Ridge National Laboratory, TN, USA
26 *Cambridge Structural Database Version 5.07* (1994) Cambridge Crystallographic Data Centre, Univ Chemical Laboratory, Cambridge, UK
27 Klyne W, Prelog V (1960) *Experientia* 16, 521–568
28 *Atlas of Steroid Structure. Vol 2* (1984) (Griffin JF, Duax WL, Weeks CM, eds) Plenum Data Company, New York, 7–11
29 Cremer D, Pople JA (1975) *J Am Chem Soc* 97, 1354–1367
30 Evans DG, Boeyens JC (1989) *Acta Cryst* B45, 581–590
31 Biosym (1994) Biosym Technologies, 10065 Barnes Canyon Rd, San Diego, CA 92121, USA
32 Al-Laham MA, Petersson GA (1991) *J Comp Chem* 12, 113–118
33 Grdiša M, Kralj M, Eckert-Maksić M, Maksić ZB, Pavelić K (1995) *J Canc Res Clin Oncol* 121, 98–102
34 Park CH (1985) *Cancer Res* 45, 3969–3973
35 Evan GI, Wyllie AH, Gilbert CS *et al* (1992) *Cell* 69, 119–128
36 Famidi A, Harrington EA, Evan GI (1992) *Nature (Lond)* 359, 554–556
37 Levine AJ, Mamand J, Finaly CA (1991) *Nature (Lond)* 351, 453–456
38 Gannon JV, Greaves R, Iggo R, Lane DP (1990) *EMBO J* 9, 1595–1602
39 Kerr JFR, Wyllie AH, Currie AR (1972) *Br J Cancer* 26, 239–257
40 Martin SJ, Green DR, Cotter TG (1994) *TIBS* 19, 26–30
41 Walker PR, Kokileva L, Le Blanc J, Sikorska M (1993) *BioTechniques* 15, 1032–1040
42 Wyllie AH (1980) *Nature (Lond)* 284, 555–556
43 Šušković B (1989) *Croat Chem Acta* 62, 537–544
44 Frenz BA & Associates Inc (1982) SDP/VAX Structure Determination Package. College Station, TX, USA
45 Sheldrick GM (1986) SHELX86. *In: Crystallographic Computing 3* (Sheldrick GM, Krueger C, Goddard R, eds) Oxford University Press
46 Sheldrick GM (1976) SHELX76, Program for Crystal Structure Determination. Univ of Cambridge, UK
47 Spek AL (1982) The EUCLID Package. *In: Computational Crystallography* (Sayre D, ed) Clarendon Press, Oxford, 528
48 Horvatić D (1992) *Byte* 3, 92IS-28
49 Allen FA, Kennard O, Wattson DG (1987) *J Chem Soc Perkin Trans* 2, S1-S19
50 Sambrook J, Fritsch EF, Maniatis T (1989) *In: Molecular Cloning: A Laboratory Manual, 2nd ed* (Nolan C, ed), Cold Spring Harbor Laboratory Press, Cold Spring Harbor, New York, 9.14-9.16
51 Pavelić K, Pavelić ZP, Denton D, Reising J, Khalily M, Preisler HD (1990) *J Exp Pathol* 5, 143–153
52 Poljak LJ, Pećina N, Džubur A, Užarevi B, Vitale B, Pavelić K (1993) *Tumordiagn Ther* 14, 158–162